Hindawi Publishing Corporation
International Journal of Polymer Science
Volume 2014, Article ID 356534, 8 pages
http://dx.doi.org/10.1155/2014/356534

Research Article

Binary Intensity Modulation and Hybrid Ternary Modulation Applied to Multiplexing Objects Using Holographic Data Storage on a PVA/AA Photopolymer

Elena Fernandez,[1,2] Rosa Fuentes,[1,2] Andrés Márquez,[2,3] Augusto Beléndez,[2,3] and Inmaculada Pascual[1,2]

[1]*Departamento de Óptica, Farmacología y Anatomía, Universidad de Alicante, Apartado 99, 03080 Alicante, Spain*
[2]*Instituto Universitario de Física Aplicada a las Ciencias y las Tecnologías, Universidad de Alicante, Apartado 99, 03080 Alicante, Spain*
[3]*Departamento de Física, Ingeniería de Sistemas y Teoría de la Señal, Universidad de Alicante, Apartado 99, 03080 Alicante, Spain*

Correspondence should be addressed to Elena Fernandez; elena.fernandez@ua.es

Received 14 July 2014; Accepted 12 November 2014; Published 10 December 2014

Academic Editor: Manuel Ortuño

Holographic data pages were multiplexed in a polyvinyl alcohol/acrylamide photopolymer and a liquid crystal device was used to modify the object beam and store objects in the material. A peristrophic multiplexing method was used to store a large number of objects in the same spot of the material. The objects were stored using two different modulations: binary intensity modulation and hybrid ternary modulation. Moreover, the bit error rate (BER) of the images was calculated in order to compare which modulation is most appropriate to be used for holographic data storage.

1. Introduction

Two-dimensional memory technologies like CD-ROMs and DVDs have arrived to their limits of capacity, and the world needs new technological systems to keep more information. Thus holographic data storage (three-dimensional technology) is becoming the new optical memory technology. These new technologies allow an important number of bits to be stored in a recording material with more capacity, more density, and faster readout rates than two-dimensional technology [1].

This work is focused on the holographic storage of objects by multiplexing in a photopolymer based on polyvinyl alcohol (PVA) and acrylamide (AA) [2] that are considered interesting materials for recording holographic memories for this high refractive index modulation and large dynamic range.

Twisted-nematic liquid crystal displays (TN-LCDs) have been applied to spatial light modulators (SLMs) to modify the amplitude or phase of a light beam in real time [3]. Another application of the nematic liquid crystals (NLC) consists of the realization of switchable holographic gratings, which leads to the intriguing possibility of the electrooptical diffractive optics. Different kinds of liquid crystalline polymer systems are suitable for these applications. The polymer dispersed liquid crystals (PDLCs) can be used for the fabrication of holographic polymer dispersed liquid crystals (HPDLCs) composed of periodic LC nano-/microdomains (droplets) separated by cross-linked polymer. Besides, the PDLCs can also be used as polymer liquid crystal slices (POLICRYPS), which are composed of slices of NLC separated by polymer walls [4–7].

However, in this paper a liquid crystal display (LCD) is used to modulate the object beam. This LCD can be used to design programmable optical elements or in holographic data storage where the LCD allows recording data pages in real time in the holographic recording material.

Moreover, two different methods for modulating the object beam are used in order to compare and select which of them is the most appropriate to store the objects: binary

Table 1: Concentrations of the photopolymer composition.

	Composition
Polyvinyl alcohol	6.6% w/v
Acrylamide	0.33 M
Triethanolamine	0.17 M
Yellowish eosin	$2.4{\cdot}10^{-4}$ M
N,N′Methylene-bis-acrylamide	0.027 M

intensity modulation (BIM) [8] and hybrid ternary modulation (HTM) [9, 10].

To generate the objects to be stored in the material, in this work a LCD was used as SLM. With a series of lenses, the Fourier transform (FT) of the objects was generated in the plane of the material which was stored by holographic techniques. As BIM produces in the FT a zero order with an intensity, several orders of magnitude higher than the other frequencies, which causes the dynamic range of the material to become saturated, other types of modulation which reduce the intensity of the zero order, for example, the HTM [11], are used to homogenize the FT.

In this work the objects were stored using these two types of modulations and the obtained results were compared to see which modulation would be the most appropriate for holographic data storage. In order to evaluate the image quality, the bit error rate [1] of each image was calculated, defined as the probability of finding bit errors in the image. Thus, images with lower BER will be the highest image quality.

2. Experimental Setup

2.1. Preparation of the Material. The holograms are recorded in a photopolymer composed of acrylamide (AA) as the polymerizable monomer, triethanolamine (TEA) as radical generator, N,N′methylene-bis-acrylamide (BMA) as crosslinker, and yellowish eosin (YE) as sensitizer and a binder of polyvinyl alcohol (PVA). Table 1 shows the component concentrations of the photopolymer composition used to obtain layers about 80 μm thick. The material is prepared with the procedure explained in [11].

2.2. Holographic Setup. A diode-pumped frequency-doubled Nd:YVO4 laser (Coherent Verdi V2) with a wavelength of 532 nm was used to record holographically the objects generated by a LCD. The laser beam was split into two beams, the object beam and the reference beam with a beam splitter. Each beam has an intensity of 1.5 mW/cm^2, and the two laser beams were spatially overlapped in the recording medium intersecting at an angle of 17.4°.

Figure 1 shows the exposures that have been used to store the objects in Figures 2 and 3. As the holograms are stored in the material, the dynamic range is consumed [1, 3, 12, 13]; therefore, the exposure must be increased in order to store more holograms. Of course, when all the dynamic range is consumed, no more holograms will be formed in the material even if the exposure is increased.

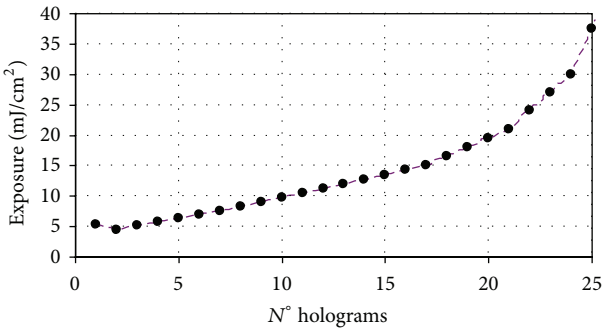

Figure 1: Exposure with which the objects of Figures 2 and 3 are recorded in the photopolymer.

The display used in this work has a resolution of 832 × 624 pixels, a pixel pitch of 32 μm, and a fill factor of 55%. The display was placed in the object beam between two polarizers and two quarter wave plates, one to each side of the LCD. In addition, a lens was placed before the first polarizer to do the Fourier transform (FT) of the object and a diaphragm was placed just before the photopolymer to block all the orders that leave the LCD except the central order. Another lens was placed behind the photopolymer to do the inverse Fourier transform (IFT) of the diffracted beam on the surface of the charge coupled device (CCD) (see [11] for more details).

2.3. Optimization of the LCD. As described in Section 2.2, an LCD was placed in the object beam to modify the wavefront and store this variation in the photopolymer. The variation of the wavefront may be in phase or amplitude. In this study, the wavefront was modified on one hand with a binary intensity modulation (BIM) [14] and on the other hand with a hybrid ternary modulation (HTM) [11, 14] in order to compare both of them.

For holographic data storage, LCDs are used as spatial light modulators to which data pages are sent to store the Fourier transform (FT) in the material by means of holographic techniques. When multiplexing objects in the same position of the material to increase its storage capacity, the monomer of the material is consumed. More or less monomer will be consumed depending on the intensity that reaches the material from the object and the reference beams. Therefore, depending on the type of used modulation, the FT of the object will be more or less intense. Generally a binary intensity modulation is used to modulate the object beam. However, when this modulation is used, the material is polymerized quickly in the area where the zero order of the FT is placed, which is more intense than the other frequencies. When a zero order of the FT is so intense, the dynamic range of the material is saturated rapidly limiting the storage of a greater amount of information. In an attempt to homogenize the FT so that there are not more intense frequencies than others, other types of modulation are used to reduce the intensity of the zero order, such as the HTM. Therefore, the main difference between the BIM and the HTM is that the BIM has a more intense zero order than the

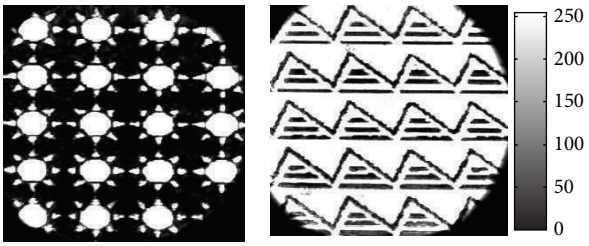

(a) (b) (c) (d)

Figure 2: ((a) and (b)) Objects that were sent to the LCD using the BIM; ((c) and (d)) corresponding images of (a) and (b) obtained illuminating the SLM with the laser beam.

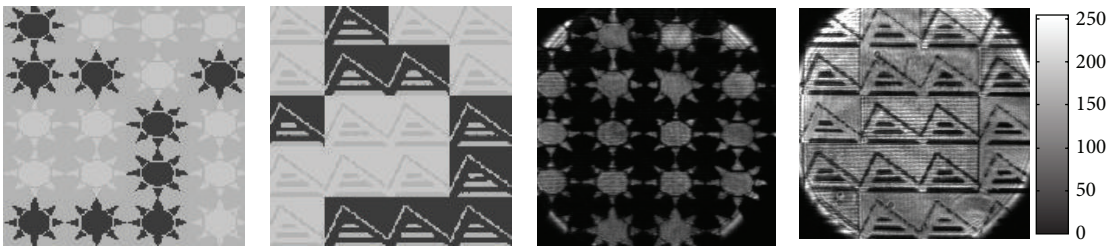

(a) (b) (c) (d)

Figure 3: ((a) and (b)) Objects that were sent to the LCD using the HTM; ((c) and (d)) corresponding images of (a) and (b) obtained illuminating the SLM with the laser beam.

other frequencies, while in the HTM all frequencies of the FT have approximately the same intensity.

By definition, the BIM has half of the bits with a transmittance value of 0 and the other half with a transmittance value of 1. On the other hand, the HTM has also half of the bits with a transmittance value of 0 and the other half with a value 1, but half of the bits with a transmittance value of 1 must have a phase difference of π rad with respect to the other half.

To create data pages with the BIM, it is necessary to find a configuration in the LCD with which the maximum contrast between transparent and opaque zones of the LCD with minimum variation in the phase was obtained. To create the objects, the grey level 250 was used to represent the bits with the maximum transmittance and the grey level 0 to represent the bits with the minimum transmittance. The justification of this choice is explained with more details in [14].

On the other hand, to create data pages with the HTM it is necessary to find a configuration in the LCD with the maximum contrast between maximum intensity bits and minimum intensity bits, so there must be a phase difference of π rad between half of the bits with maximum intensity and the other half. To create the objects, the grey levels 200 and 60 were used to represent the bits with the maximum transmittance having a phase difference of π rad between them, whereas the grey level 150 was used to represent the bits with the minimum transmittance. The justification to choose these values is explained with more details in [11, 14].

3. Results

With the experimental setup in Section 2.2, two objects were multiplexed, each with a different set drawing. Specifically, the figure of a sun and the logo of the University of Alicante were stored. These two objects were chosen because black pixels are predominant in the first one and white pixels are predominant in the second one and thus it is possible to compare the results obtained with each of these two objects. The objects were modulated with the configurations of the Section 2.3 (BIM and HTM). Moreover, they were multiplexed using a peristrophic multiplexing with an angular separation between holograms of 5°.

3.1. Original Images. Figures 2(a) and 2(b) show the objects that were sent to the LCD using the BIM. These objects are made with two grey levels, 0 and 250, which provide the contrast maximum, as discussed in Section 2.3. Figures 2(c) and 2(d) show the corresponding images of these objects which were captured by the CCD camera when the SLM was illuminated by the laser beam. As it can be observed, these images have good contrast between black and white pixels.

Figures 3(a) and 3(b) show the objects that were sent to the LCD using the HTM. The objects are formed by three grey levels, the grey levels 60 and 200 which have a maximum transmittance and have a phase shift of π rad and the grey level 150 which has a minimum transmittance. Figures 3(c) and 3(d) show the corresponding images of these objects which were captured by the CCD camera when the SLM was illuminated by the laser beam. As can be seen in Figure 3(a),

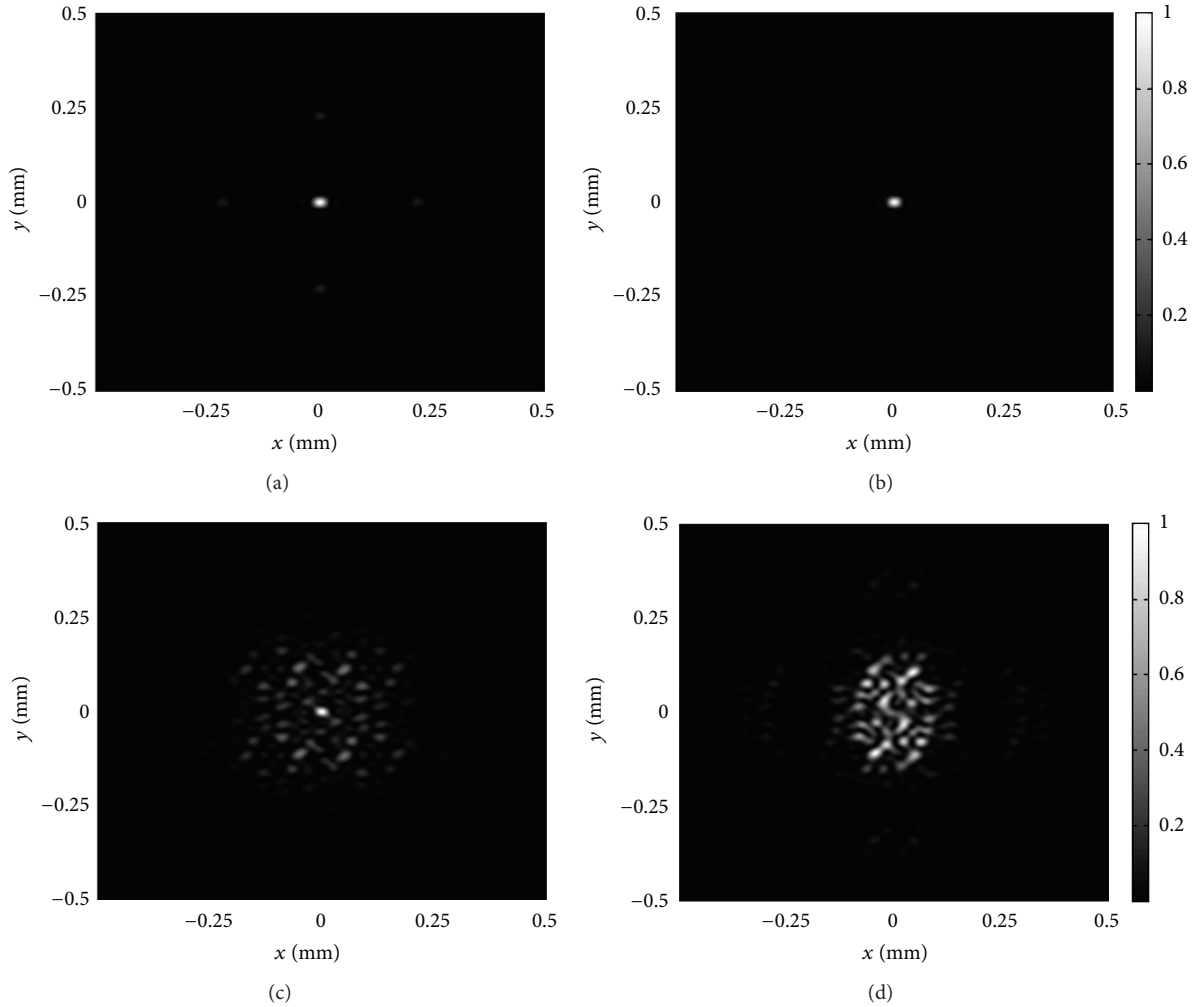

Figure 4: Far field diffraction patterns at a distance of 1 m of (a) binary image depicted in Figure 2(a); (b) binary image depicted in Figure 2(b); (c) hybrid ternary image depicted in Figure 3(a); and (d) hybrid ternary image depicted in Figure 3(b).

the pictures of the sun are drawn with the two grey levels, but, in Figure 3(c), all the pictures of the sun have the same maximum transmittance; the background in Figure 3(a) has a certain grey level, but in Figure 3(c) the background has a minimum transmittance. The same occurs for Figures 3(b) and 3(d). This happens thanks to the SLM which is optimized to generate this configuration.

An important fact that has to be highlighted because it can influence the final results is that if the images obtained with BIM and the HTM are compared, it can be observed that the latter have a lower contrast because the bits that represent the maximum transmittance in HTM have a lower transmittance than the same bits in BIM.

3.2. Far Field Diffraction Patterns. Figures 4(a)–4(d) show the far field diffraction patterns corresponding to the images depicted in Figures 2(a), 2(b), 3(a), and 3(b), respectively. Such diffraction patterns have been calculated through the Fraunhofer diffraction formula at a distance of 1 m from the object planes, and the intensities have been normalized to unity. In the case of the far field pattern of the binary image depicted in Figure 2(a), Figure 4(a) shows a dominant diffraction order at the centre of the image together with less intense diffraction orders. These secondary diffraction orders can be explained taking into account that the pattern depicted in Figure 2(a) is similar to a finite size array of ordered circular slits with spatial periods in accordance with the corresponding diffraction orders. However, Figure 4(b) shows that the far field pattern of the binary image depicted in Figure 2(b) has a dominant central diffraction order with the secondary orders being negligible. This is due to the fact that the pattern depicted in Figure 2(b) is more complex and differs from the aforementioned array of ordered slits.

On the other hand, Figures 4(c) and 4(d) show that the far field diffraction patterns of the hybrid ternary images depicted in the respective Figures 3(a) and 3(b) are more complex, and the previous central diffraction order now spreads covering a wider region. This is the expectable result taking into account that the images shown in Figures 3(a) and 3(b)

have three levels both in amplitude and phase, which necessarily implies a wider band of spatial frequencies.

3.3. Bit Error Rate. In this section, the objects of Figure 2 with the BIM and Figure 3 with the HTM were multiplexed. After one of the objects had been stored in the photopolymer, the hologram formed was reconstructed illuminating it with the reference beam. The diffractive beam obtained was imaged onto the CCD. However, the image may be distorted for many reasons; therefore, it is advisable to measure a parameter that quantifies the image quality. This parameter is the bit error rate (BER).

The BER is defined as the probability of having erroneous bits in the image. To calculate the BER, the probability of obtaining a certain gray level in the black or in the white regions must be calculated, that is, the histogram of the black bits and the histogram of the white bits, respectively. The two probability distributions intersect in a point called x_c. Then both distributions are fitted to a Gaussian equation [15, 16]:

$$W(x_0, \sigma; x) = \frac{1}{\sqrt{2\pi\sigma}} \exp\left(-\frac{(x - x_0)^2}{2\sigma^2}\right), \quad (1)$$

where x represents each gray level in the image, x_0 is the point at which the Gaussian distribution is centered, and σ is the width of the Gaussian distribution. Finally, with the adjustments for the probability distribution of both white and black bits, BER is calculated from

$$\text{BER} = \frac{1}{2}\left[\int_0^{x_c} W_W(x)\,dx + \int_{x_c}^{\infty} W_B(x)\,dx\right], \quad (2)$$

where W_W and W_B are the adjustments of the probability distribution of white and black pixels, respectively, and x_c is the point of intersection of the two probability distributions.

The lower the BER of the stored images, the greater their quality. But how can we tell if an image is of good quality? In a previous study [15] it was found that images with a value of BER less than or equal to 0.2 still had good contrast and well-defined edges; that is, they were images of acceptable quality. Therefore, a BER of 0.2 is taken as the threshold value below which the images obtained are considered to be of good quality.

Figure 5 shows the BER values that were obtained by storing the two objects with the two modulations (Figures 2 and 3). BER values of the object of the SUN stored with BIM are represented with red squares. As shown, 20 holograms are stored; the first 13 holograms have a BER less than 0.1, and the holograms 14 to 20 have values of BER of 0.2. After that, BER values of the SUN stored with HTM are represented with black circles. As can be seen, 24 holograms have been stored with a BER value lower than 0.2, although the BER values are slightly higher than those obtained with the BIM for the first 13 holograms.

Moreover, Figure 5 represents the BER values of the object of the LOGO UA stored with BIM with blue squares. 20 holograms have been stored with BER values lower than 0.2, but slightly higher than the BER values obtained with the object of the SUN for the same modulation. In addition,

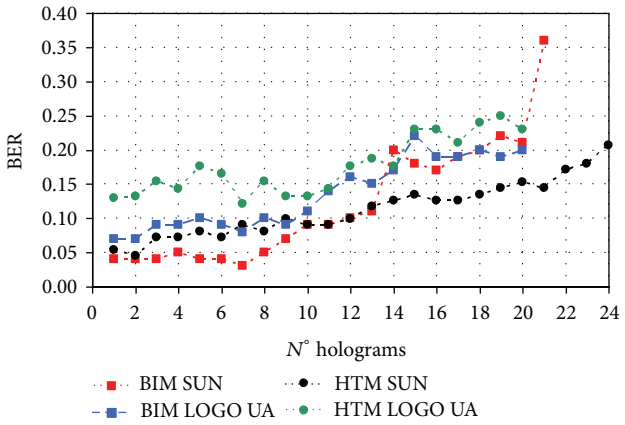

Figure 5: BER values obtained multiplexing the object of SUN and LOGO UA for the BIM and HTM.

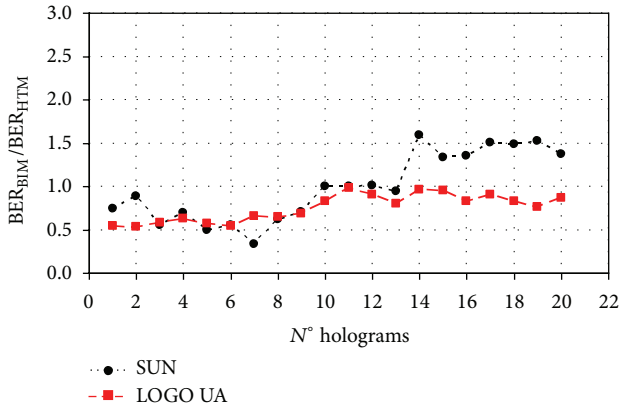

Figure 6: Relative values of the BER between the BIM and HTM for the objects of SUN and LOGO UA.

15 holograms have been stored with BER values lower than 0.2 for the LOGO UA stored with HTM. These values are represented with green circles in Figure 5.

If all the results shown in Figure 5 are compared, it is observed that, with the object of the SUN, 20 holograms were multiplexed with the BIM and 24 holograms were multiplexed with the HTM with BER values lower than 0.2. And, with the object of the LOGO UA, 20 holograms were multiplexed with the BIM and 15 holograms were multiplexed with the HTM with BER values lower than 0.2. Therefore, 20 holograms have been multiplexed with the two different objects with the BIM. So, the type of object that is multiplexed does not significantly influence the results since, regardless of the object having mostly white bits or black bits, the same number of holograms is multiplexed. However, this fact does not occur with the HTM, since 24 holograms with BER values lower than 0.2 were multiplexed with the object of the SUN, but with the object of LOGO UA only 15 holograms were multiplexed with BER values lower than 0.2.

In order to obtain a better comparison between the two modulations, relative BER has been calculated dividing the BER of the BIM over the BER of the HTM for the objects of SUN and LOGO UA. Figure 6 represents the obtained

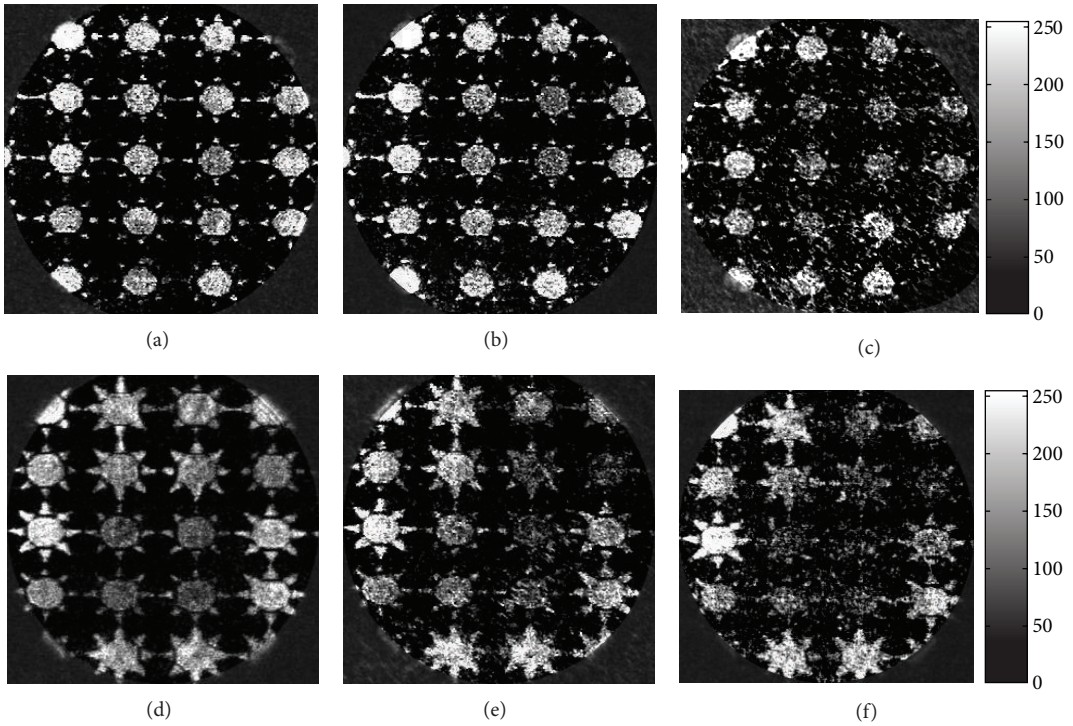

Figure 7: Object of SUN: ((a), (b), and (c)) images of the holograms numbers 1, 5, and 15, respectively, stored with BIM. ((d), (e), and (f)) Images of the holograms numbers 1, 5, and 15, respectively, stored with HTM.

values for the relative BER. As it can be seen, the relative BER is lower than 1 for the 9 first holograms and for both objects. This means that the quality of the image for these nine holograms is better for the BIM than for the HTM. Moreover, for the object of LOGO UA, the relative BER is near 1 for holograms 10 to 20. This means that, for these holograms, both modulations provide more or less the same image quality. However, for the object of the SUN, the relative BER is the same for holograms 10 to 13, but it is higher than 1 for holograms 14 to 20. This means that, for these holograms, the HTM provides a better image quality than the BIM in the object of the SUN.

Figure 7 shows the images of the SUN stored with BIM (Figures 7(a), 7(b), and 7(c) corresponding to holograms 1, 5, and 15, resp.) and the images of the SUN stored with the HTM (Figures 7(d), 7(e), and 7(f), corresponding to holograms 1, 5, and 15). The more important difference when the same object is stored with the two studied modulations is that a higher resolution is obtained with the BIM than with the HTM. It can be observed that with the BIM there are some black spaces between the centre of the sun and the sunrays which are not distinguished so clearly with the HTM.

Figure 8 shows the images of the LOGO UA stored with BIM (Figures 8(a), 8(b), and 8(c) corresponding to holograms 1, 5, and 15 resp.) and the images of the LOGO UA stored with the HTM (Figures 8(d), 8(e), and 8(f) corresponding to holograms 1, 5, and 15). If images with BIM and HTM are compared, it is important to highlight that these last three images have higher noise, lower contrast, and lower resolution than the images stored with the BIM.

When Figures 7 and 8 are compared it can be noticed that images of Figure 8 have more noise than images of Figure 7. It is probably because the images of the LOGO UA have more white areas than the SUN.

3.4. Diffraction Efficiency. The diffraction efficiency (DE) of the multiplexed images for the two objects and the two modulations has also been calculated dividing the intensity of the diffracted beam by the intensity of the incidence beam (reference beam). Figure 9 shows the DE of the SUN obtained with the BIM with red squares and the one obtained with the HTM with black circles. In addition, Figure 9 shows the DE of the LOGO UA obtained with the BIM with blue squares and the one obtained with the HTM with green circles.

As it can be seen, for the object of the SUN, the DE obtained with the BIM is higher than the DE obtained with the HTM for the first 11 holograms. Besides, hologram 12 has the same DE for both modulations, and the DE in holograms 13 to 24 is higher for the HTM than for the BIM.

However, for the object of LOGO UA, the DE obtained with the BIM is higher than the DE obtained with the HTM for all the holograms.

4. Conclusions

In this study, two different objects were multiplexed in layers of PVA-acrylamide photopolymer with a thickness of 80 μm. TN-LCDs were used as a spatial light modulator to modify the object beam and store the data pages in the material. The BER of the multiplexed images was calculated to quantify

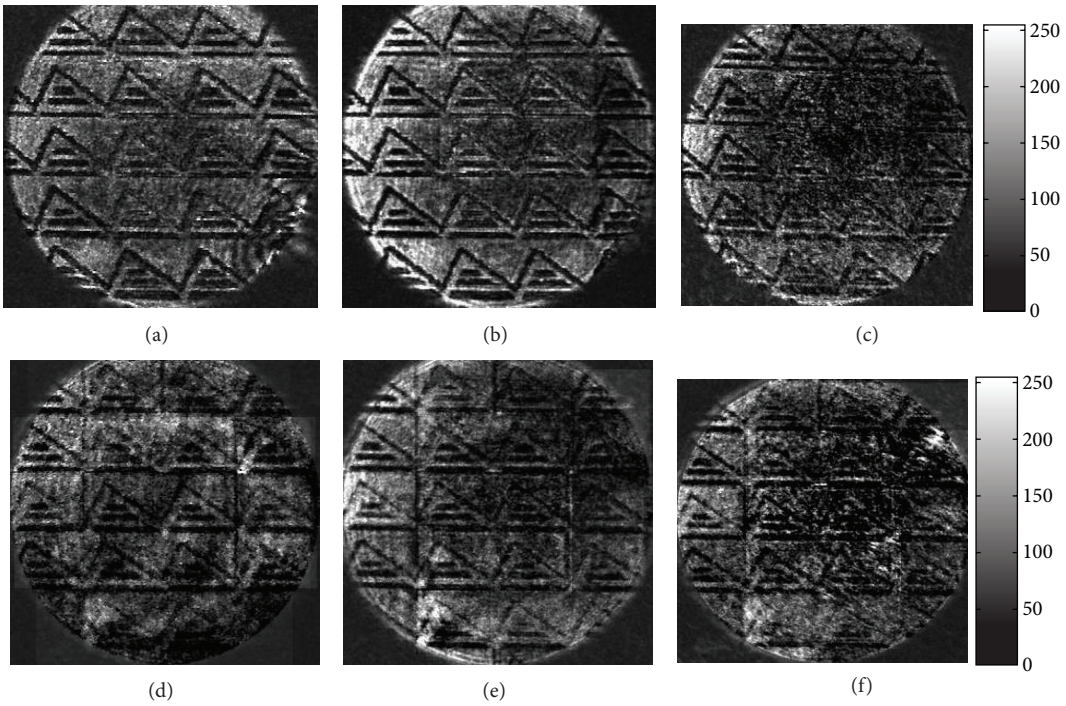

Figure 8: Object of LOGO UA: ((a), (b), and (c)) images of the holograms numbers 1, 5, and 15, respectively, stored with BIM. ((d), (e), and (f)) Images of the holograms numbers 1, 5, and 15, respectively, stored with HTM.

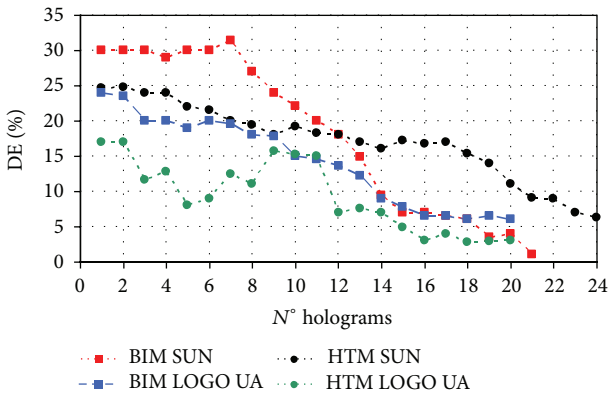

Figure 9: DE versus the hologram number for the objects of the SUN and LOGO UA for the BIM and the HTM.

the quality of the images and represented versus the number of multiplexed holograms.

Two different configurations were used to modulate the object beam with a LCD: the binary intensity modulation (BIM) and the hybrid ternary modulation (HTM). The BIM produces a high zero frequency which may saturate the dynamic range of the material and limit the accessible dynamic range. In order to reduce the zero frequency of the FT of the objects, HTM was used to modulate the object beam. Reducing this zero frequency, more holograms were superimposed at the same position in the material than with the BIM. However, when storing objects with any drawing, to get more details on these objects, it is advisable to store them with BIM.

Therefore, it is concluded that, regardless of the modulation used, the best results are achieved with objects in which white bits are not predominant (i.e., objects with half of the bits white and half of the bits black), since the images obtained with these features have a lower noise and, moreover, if the HTM is used, a larger number of holograms are multiplexed with this type of objects.

Thus, the configuration with which the greatest number of holograms has been obtained was the HTM with the object of the SUN. However, if you want to multiplex any type of objects, regardless of the density of the white bits, or if you want to multiplex only a few objects but with very high image quality, it is preferable to use the BIM.

Conflict of Interests

The authors declare that there is no conflict of interests regarding the publication of this paper.

Acknowledgments

This work was supported by the "Generalitat Valenciana" (Spain) under Projects PROMETEO/2011/021 and ISIC/2012/013 and by "Ministerio de Ciencia e Innovación" (Spain) under Projects FIS2011-29803-C02-01 and FIS2011-29803-C02-02.

References

[1] H. Coufal, D. Psaltis, and G. T. Sincerbox, *Holographic Data Storage*, Springer, New York, NY, USA, 2000.

[2] M. R. Gleeson, J. V. Kelly, C. E. Close, F. T. O'Neill, and J. T. Sheridan, "Effects of absorption and inhibition during grating formation in photopolymer materials," *Journal of the Optical Society of America B: Optical Physics*, vol. 23, no. 10, pp. 2079–2088, 2006.

[3] L. Dhar, K. Curtis, M. Tackitt et al., "Holographic storage of multiple high-capacity digital data pages in thick photopolymer systems," *Optics Letters*, vol. 23, no. 21, pp. 1710–1712, 1998.

[4] R. L. Sutherland, L. V. Natarajan, V. P. Tondiglia, and T. J. Bunning, "Bragg gratings in an acrylate polymer consisting of periodic polymer-dispersed liquid-crystal planes," *Chemistry of Materials*, vol. 5, no. 10, pp. 1533–1538, 1993.

[5] L. De Sio, N. Tabiryan, and T. Bunning, "Spontaneous radial liquid crystals alignment on curved polymeric surfaces," *Applied Physics Letters*, vol. 104, Article ID 221112, 2014.

[6] L. de Sio, S. Ferjani, G. Strangi, C. Umeton, and R. Bartolino, "Soft periodic microstructures containing liquid crystals," *The Journal of Physical Chemistry B*, vol. 117, no. 4, pp. 1176–1185, 2013.

[7] S. C. Jain and D. K. Rout, "Electro-optic response of polymer dispersed liquid-crystal films," *Journal of Applied Physics*, vol. 70, no. 11, pp. 6988–6992, 1991.

[8] J. Joseph and D. A. Waldman, "Homogenized Fourier transform holographic data storage using phase spatial light modulators and methods for recovery of data from the phase image," *Applied Optics*, vol. 45, no. 25, pp. 6374–6380, 2006.

[9] R. John, J. Joseph, and K. Singh, "Holographic digital data storage using phase-modulated pixels," *Optics and Lasers in Engineering*, vol. 43, no. 2, pp. 183–194, 2005.

[10] J. Reményi, P. Várhegyi, L. Domján, P. Koppa, and E. Lõrincz, "Amplitude, phase, and hybrid ternary modulation modes of a twisted-nematic liquid-crystal display at ~400 nm," *Applied Optics*, vol. 42, no. 17, pp. 3428–3434, 2003.

[11] E. Fernández, A. Márquez, S. Gallego, R. Fuentes, C. García, and I. Pascual, "Hybrid ternary modulation applied to multiplexing holograms in photopolymers for data page storage," *Journal of Lightwave Technology*, vol. 28, no. 5, Article ID 5398921, pp. 776–783, 2010.

[12] P. Várhegyi, P. Koppa, F. Ujhelyi, and E. Lorincz, "System modeling and optimization of Fourier holographic memory," *Applied Optics*, vol. 44, no. 15, pp. 3024–3031, 2005.

[13] E. Fernández, M. Ortuño, S. Gallego, C. García, A. Beléndez, and I. Pascual, "Comparison of peristrophic multiplexing and a combination of angular and peristrophic holographic multiplexing in a thick PVA/acrylamide photopolymer for data storage," *Applied Optics*, vol. 46, no. 22, pp. 5368–5373, 2007.

[14] E. Fernández, A. Márquez, M. Ortuño, R. Fuentes, C. García, and I. Pascual, "Optimization of twisted-nematic liquid crystal displays for holographic data storage," *Optica Pura y Aplicada*, vol. 42, no. 3, pp. 125–132, 2009.

[15] E. Femández, M. Ortuño, S. Gallego et al., "Multiplexed holographic data page storage on a polyvinyl alcohol/acrylamide photopolymer memory," *Applied Optics*, vol. 47, no. 25, pp. 4448–4456, 2008.

[16] J. Ashley, M.-P. Bernal, G. W. Burr et al., "Holographic data storage," *IBM Journal of Research and Development*, vol. 44, no. 3, pp. 341–368, 2000.